Magnetic behavior of stoichiometric and nonstoichiometric GdAs single crystals

D. X. Li,* Y. Haga, H. Shida, and T. Suzuki
Department of Physics, Tohoku University, Sendai 980-77, Japan

T. Koide and G. Kido
Institute for Materials Research, Tohoku University, Sendai 980-77, Japan
(Received 11 May 1995)

The magnetizations, magnetic susceptibilities, and specific heats of both stoichiometric and nonstoichiometric single crystals GdAs are measured at temperatures $1.7 \leqslant T \leqslant 300$ K and magnetic fields $0 \leqslant H \leqslant 24$ T. A systematic comparison between the magnetic behavior of the stoichiometric and nonstoichiometric samples is carried out. The stoichiometric sample shows the magnetic features expected for a Heisenberg antiferromagnet. For the nonstoichiometric sample, some anomalous magnetic properties are observed and explained by the trapped magnetic polaron model.

I. INTRODUCTION

Rare-earth monopnictides RX ($X=$ N, P, As, Sb, and Bi) with NaCl-type crystal structure are the most typical materials in low carrier systems. Much attention has been attracted on these materials, due to their mysterious magnetic and transport properties. Recently, the success in preparing many high quality RX single crystals has made much progress in experimental studies of these compounds, in particular, in La, Ce, and Yb monopnictides. Although the experimental results are not sufficient, various complicated physical phenomena such as the dense Kondo effect, valence fluctuations, heavy fermions state, magnetic exchange interactions, crystalline-electric field (CEF) effect and magnetic polaron effect, etc., have been observed in RX systems. Different effects exist in different samples and compete with each other, thus the RX systems show diverse physical properties. Although some of the anomalous properties are explained by Kasuya *et al.*,[1–5] there are still many unsolved issues in these systems. Understanding the mechanism of these effects is the prerequisite of explaining the anomalous physical properties of RX systems.

First, much attention has been focused on the magnetic exchange interactions between $4f$ ions due to their important role in most rare-earth monopnictides. The direct exchange interaction due to direct $4f$-$4f$ overlap between nearest-neighbor sites in the RX systems is weak, because the $4f$ electrons are well screened by $5s$ and $5p$ closed shells. Therefore, in most cases indirect exchange interaction must be the main mechanism. The media of the indirect exchange interaction between $4f$ spins are believed to be the intra-atomic d-f interaction, and d-f or p-f mixing interaction (where "d" represents the conduction election, i.e., $5d$ or $6s$ electrons in rare-earth atoms, "p" represents the p-band hold of pnictogen).[6] The former contains the isotropic d-f Coulomb interaction, the isotropic d-f exchange interaction, and the multipole and anisotropic exchange interactions. For studying the indirect exchange interaction in RX systems more thoroughly, it is desirable to have a "model" material exhibiting the exchange effect only. This is fulfilled by the behavior of GdAs, one of the NaCl structure compounds of RX systems with low carrier concentration. Because Gd^{3+} with $4f^7$ configuration is an S-state ion with spin-7/2, CEF effects in GdAs are expected to be fairly weak and the indirect exchange interaction is the main mechanism, while the anisotropic exchange and the multipole interactions are negligible in GdAs. Furthermore, the $4f$ level in GdAs is sufficient below the Fermi energy and therefore d-f or p-f mixing can also be neglected in GdAs. On the whole, GdAs is the most suitable material to study the indirect exchange mechanism in RX systems by using the d-f Coulomb exchange interaction. On the other hand, since GdAs is the "exchange only" system with low carrier concentration, the so-called trapped magnetic polaron states can be formed easily which affects the magnetic and transport properties of GdAs strongly. However, because of the difficulty of growing GdAs single crystal, the experiment studies have not been done in detail. Recently, we have succeeded in growing large stoichiometric and nonstoichiometric GdAs single crystals and carefully measured the physical properties. In this paper, we will systematically compare the magnetic properties between the two samples, one is noted as GdAs No. 1, the nonstoichiometric single crystal, and another is noted as GdAs No. 2, the stoichiometric single crystal. The experiments will be discussed with molecular field approximation (MFA) and the trapped magnetic polaron model. The electrical transport behavior of them will be analyzed in a separate paper.

II. SAMPLE PREPARATION AND EXPERIMENT

Single crystals of GdAs No. 1 and GdAs No. 2 are grown by the mineralization method in tungsten crucibles. Because arsenic is easy to evaporate at high temperature, a prereaction of the constituent elements, Gd and As, is first carried out in a closed quartz ampoule at 550 °C for six weeks. The Gd metal of 99.9% purity (turned into small flakes in a glovebox permeated with Ar gas) and As metal of 99.999% purity are used. The polycrystalline materials of GdAs No. 1 and GdAs No. 2 obtained by the prereaction are pressed into hard pellets at 720 °C and 1300 atm using a glass capsule method. The hard pellets are then sealed in cleared tungsten crucibles using an electron beam gun in vacuum. Finally the

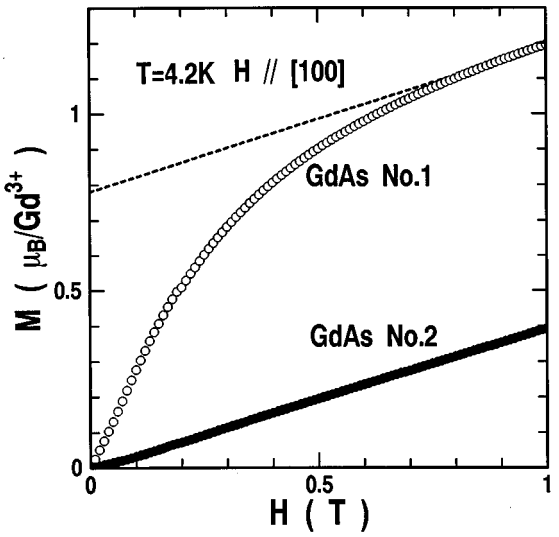

FIG. 1. Magnetic field dependence of the magnetization of GdAs No. 1 and GdAs No. 2 measured at $T=4.2$ K and $H\leqslant 1$ T. The dashed line is extrapolation of the data above 0.8 T to lower fields for GdAs No. 1.

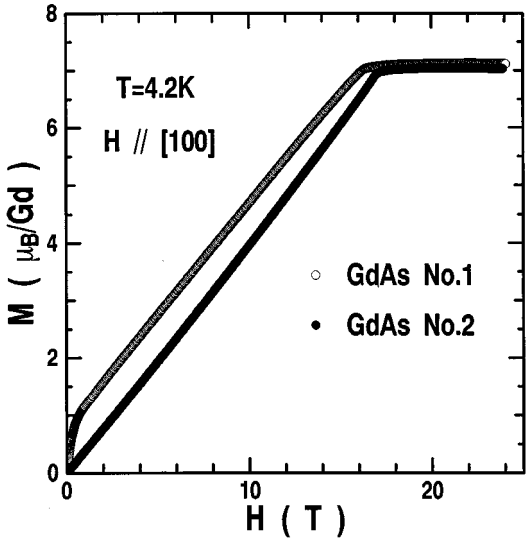

FIG. 2. Magnetic field dependence of the magnetization of GdAs No. 1 and GdAs No. 2 measured at $T=4.2$ K and $H\leqslant 24$ T.

crucibles are slowly heated to above 2500 °C, using a high-frequency induction furnace and kept at this temperature for 72 h. By this method, single crystals of GdAs No. 1 and GdAs No. 2 with dimensions of about $8\times6\times6$ mm^3 and $5\times5\times5$ mm^3, respectively, have been obtained. The x-ray-diffraction patterns show single phases of NaCl-type GdAs for both samples. The room-temperature lattice constants a are 5.895(1) Å for GdAs No. 1 and 5.864(1) Å for GdAs No. 2. The atomic ratios between Gd and As determined by chemical analysis are $1:0.95\pm0.01$ for GdAs No. 1 and $1:1.00\pm0.01$ for GdAs No. 2, respectively. Thus GdAs No. 1 is a nonstoichiometric sample and GdAs No. 2 is a stoichiometric sample.

The samples used for various measurements are cut from the large single crystals. The high-field magnetization M is measured by using a pulse magnetic field ($0\leqslant H\leqslant 24$ T), while the low-field magnetization ($H\leqslant 1$ T) is measured in detail with a Quantum Design superconducting quantum interference device (SQUID) magnetometer. The susceptibility χ is measured as a function of magnetic field H of $0.05<H<1$ T and temperature T of $1.7<T<300$ K, respectively, with the Quantum Dedign SQUID magnetometer the same as that used for low-field magnetization measurements. The specific heat measurements are carried out with an adiabatic method at temperature of $1.7<T<60$ K and magnetic field of $0\leqslant H\leqslant 10$ T.

III. RESULTS

A. Magnetization

The low-field magnetization curves measured by increasing magnetic field are displayed in Fig. 1. The measurements are carried out at $T=4.2$ K and $\boldsymbol{H}\parallel[100]$ direction. In the nonstoichiometric sample GdAs No. 1 the magnetization shows a rapid increase at small fields and a linear field dependence above 0.8 T. Extrapolation of the H-linear part of the magnetization curve, shown by dashed line in Fig. 1, intercepts with the M axis at $0.78\mu_B/\mathrm{Gd}^{3+}$. Compared to the saturation moment of a free Gd^{3+} ion, $M_s=7.0\mu_B/\mathrm{Gd}^{3+}$, this value corresponds to about $M_s/10$. The nonlinear increase of the magnetization at low field suggests the existence of weak ferromagnetism, i.e., the presence of a spontaneous magnetic moment at zero field. Magnetization measurements by increasing and decreasing fields reveal no hysteresis behavior for GdAs No. 1. For the stoichiometric sample GdAs No. 2 similar extrapolated straight line, which are not shown in Fig. 1, intercepts with the H axis at about 0.02 T. This suggests that the anisotropy field is very small for GdAs No. 2.

Figure 2 shows the high-field magnetizations up to 24 T measured at $T=4.2$ K with $\boldsymbol{H}\parallel[100]$ direction for the two samples. For a given H, the magnetization for GdAs No. 1 is slightly higher than that for GdAs No. 2. The saturation field and saturation moment are about 18 T and $7.01\mu_B/\mathrm{Gd}^{3+}$, respectively, for the stoichiometric sample GdAs No. 2, and about 17 T and $7.06\mu_B/\mathrm{Gd}^{3+}$, respectively, for the nonstoichiometric sample GdAs No. 1.

The H dependencies of dM/dH of GdAs No. 1 and GdAs No. 2 are illustrated in Fig. 3. The inset of this figure shows the low-field results. At low fields, dM/dH in GdAs No. 2 first increases as H increases, then goes through a broad maximum centered at 0.16 T, and finally reaches a constant value $\chi_\perp=0.223$ emu/mol. This values agrees with $\chi_{\max}=0.225$ emu/mol, the maximum value of the susceptibility of stoichiometric sample GdAs No. 2 described in the following. This broad peak relates to the spin-flop transition analogous to the case in uniaxial antiferromagnet.[7] This feature will be discussed in detail in Sec. IV. Above 3 T, dM/dH increases very slowly, and at $H=H_C=16.7$ T, the dM/dH curve exhibits a λ peak, while above H_C, dM/dH drops abruptly. This λ peak indicates a phase transition from canted phase to paramagnetic phase. In GdAs No. 1, the values of dM/dH at low fields are much larger than those in sample GdAs No. 2. Starting at $H=0$, dM/dH of GdAs No. 1 first increases, then passes through a maximum at about 0.07 T, and finally reduces rapidly and reaching the constant

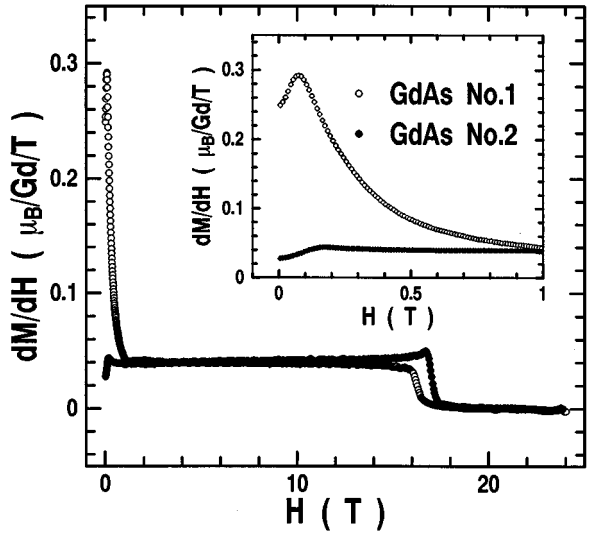

FIG. 3. Differential susceptibility dM/dH vs applied magnetic field for GdAs No. 1 and GdAs No. 2 at 4.2 K. The inset shows details below 1 T.

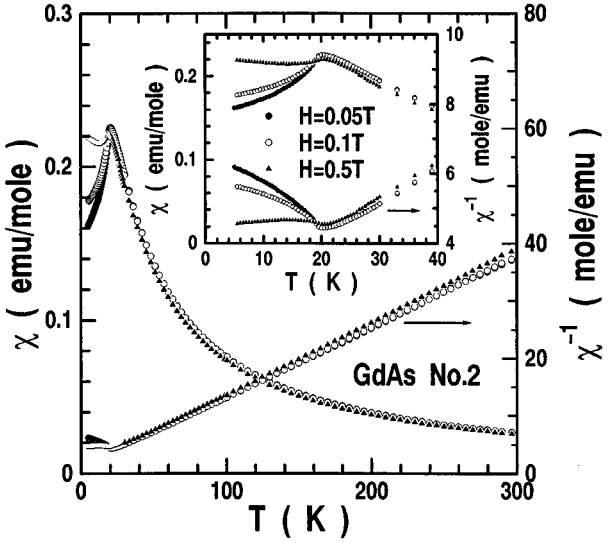

FIG. 4. Temperature dependencies of the susceptibility and the inverse susceptibility of GdAs No. 2 measured in magnetic fields of 0.05, 0.1, and 0.5 T. The inset is the low-temperature part.

approaching $\chi_\perp$ at about 1 T. Above 1 T, dM/dH remains a constant value up to 15 T. The peak appeared at 0.07 T in GdAs No. 1 relates to the saturation field of the weak ferromagnetism. This feature will be also discussed in detail in Sec. IV. The rapid dropping of dM/dH associated with the transition from the canted phase to paramagnetic phase also occurs at $H_C=16$ T in nonstoichiometric sample GdAs No. 1; however, a significant difference between the two dM/dH curves is that the λ anomaly at H_C in GdAs No. 1 is less obvious compared with GdAs No. 2.

B. Magnetic susceptibility

Magnetic susceptibility χ and inverse susceptibility $1/\chi$ measured at different fields ($\boldsymbol{H}\|[100]$) are presented in Figs. 4 and 5 versus temperature for GdAs No. 2 and GdAs No. 1, respectively. The low temperature behaviors are shown in the insets of these figures. The stoichiometric and nonstoichiometric samples show clearly different behaviors. The main features of sample GdAs No. 2 are the following. (1) The susceptibility is Curie-Weiss-like at higher temperatures, as can be seen from the inverse susceptibility. Using the expression $\chi=C/(T-\theta_P)$, here $C=N_A\mu_{\rm eff}^2/(3k_B)$, the best fit of the data above 100 K yields $\theta_P=-11.5$ K and $\mu_{\rm eff}=8.15\mu_B$. (2) The susceptibility starts to deviate from the Curie-Weiss behavior at about 100 K. The Néel temperature is identified as the temperature of the peak in $d(T\chi)/dT$ which gives $T_N=18.7$ K for all three curves corresponding to the fields of 0.05, 0.1, and 0.5 T. Note that the maximum in χ occurs just above T_N, and near T_N, the intensity of the peak in χ decreases with the increasing field. (3) Below T_N, the χ-H dependence shows that χ increases with H and this increase becomes rapid with the decreasing temperature, while the χ-T dependence shows that χ reduces quickly with the decreasing T at $H=0.05$ and 0.1 T. At $H=0.05$ T, the χ reduces to 0.162 emu/mol at 5 K; this value is close to $2/3\chi_{\rm max}$, where $\chi_{\rm max}=0.225$ emu/mol is the maximum value of χ reached just above T_N. In $H=0.5$ T, however, the susceptibility shows the behavior different from those of $H=0.05$ and 0.1 T, e.g., below T_N, as the temperature decreases, χ first reduces, then passes through a shallow minimum, and finally increases. From T_N to room temperature, its value is slightly lower than the value of $H=0.05$ and 0.1 T. Compared with GdAs No. 2, the nonstoichiometric sample GdAs No. 1 shows very different susceptibility behavior. (1) Although χ follows the Curie-Weiss law at higher temperature, a positive paramagnetic Curie temperature $\theta_P=19.4$ K and a effect moment $\mu_{\rm eff}=8.04\mu_B$ are obtained by the best fitting of the data above 100 K. (2) χ starts to deviate from the Curie-Weiss behavior at about 100 K, similar to that in GdAs No. 2. However, at about 17 K only a small bend appears in χ curve. The small bend is also the characteristic of an antiferromagnetic phase transition despite

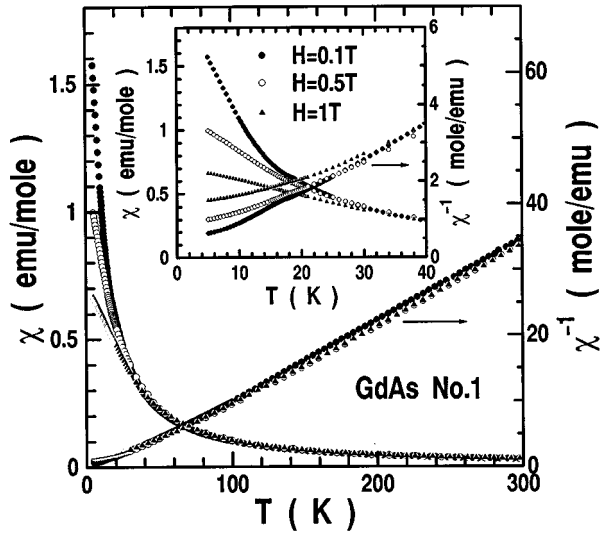

FIG. 5. Temperature dependencies of the susceptibility and the inverse susceptibility of GdAs No. 1 measured in magnetic fields of 0.1, 0.5, and 1 T. The inset is the low-temperature part.

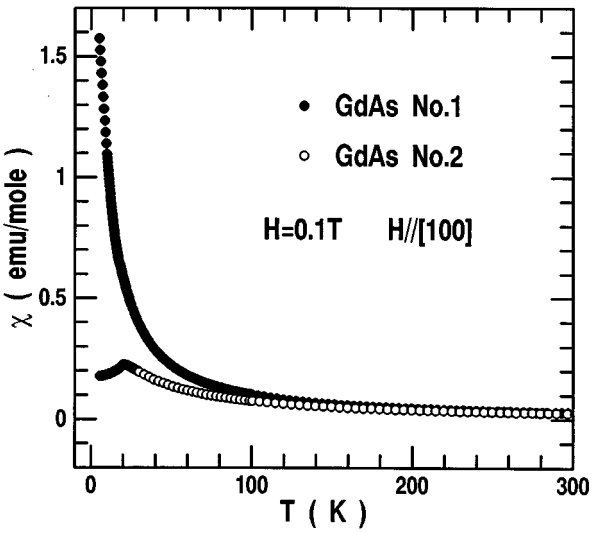

FIG. 6. Temperature dependence of the susceptibility for GdAs No. 1 and GdAs No. 2 measured in a field of 0.1 T.

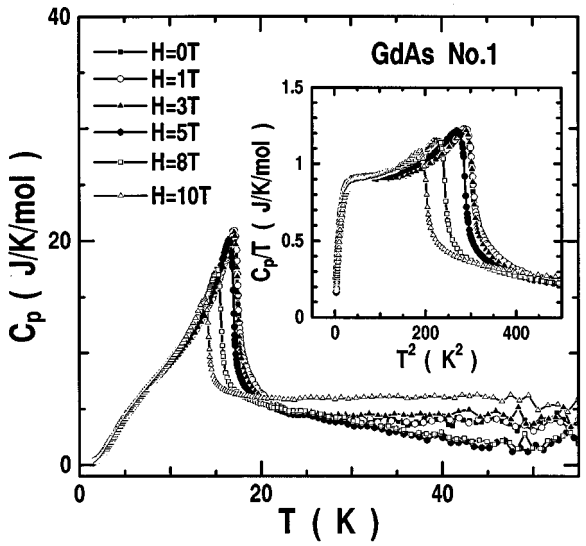

FIG. 7. Temperature dependence of the magnetic part of the specific heat of GdAs No. 1 in magnetic fields of 0, 1, 3, 5, 8, and 10 T. The inset shows the behavior of C_P/T versus T^2.

that it is not a sharp transition peak. From the derivative $d(T\chi)/dT$, we observe a peak at $T_N=17.2$ K. (3) At low temperature, the χ-H behavior is on the contrary to that of stoichiometric sample GdAs No. 2, that is χ reduces as the field increases up to 1 T. Even at T_N, the deviation of χ values between different fields is also evident. Note that, as can be seen in Fig. 6, at low temperatures, susceptibility in the nonstoichiometric GdAs No. 1 is much higher than that in the stoichiometric GdAs No. 2 due to the existence of weak ferromagnetism in GdAs No. 1. This deviation becomes smaller gradually with the increasing T and disappears above 200 K. Compared with the large disparity (about 33 K) of the paramagnetic Curie temperature θ_P, only a smaller disparity (about 1.5 K) of the Néel temperature T_N[T_N is determined as the temperature where $d(T\chi)/dT$ has the maximum value, which gives $T_N=18.7$ K for GdAs No. 2 and $T_N=17.2$ K for GdAs No. 1] between the two samples is observed.

C. Specific heat under magnetic fields

Figures 7 and 8 show the magnetic parts of specific heat [obtained by subtracting the data of $(C_{\mathrm{LaAs}}+C_{\mathrm{LuAs}})/2$ from $C_{\mathrm{GdAs\ No.1}}$ and $C_{\mathrm{GdAs\ No.2}}$] measured in magnetic fields up to 10 T for GdAs No. 1 and GdAs No. 2, respectively. At zero field, an antiferromagnetic transition peak is observed at 18.7 K for GdAs No. 2 and 17.2 K for GdAs No. 1; these values are in good agreement with the susceptibility measurements. For both samples, as H increases, the intensity of this peak decreases and the peak position shifts gradually to lower temperature. In GdAs No. 2, the peak position shifts from 18.7 K at $H=0$ to 15.5 K at $H=10$ T, and in GdAs No. 1, the peak position shifts from 17.2 K at $H=0$ to 13.9 K at $H=10$ T. Compared with GdAs No. 2, the transition peaks of GdAs No. 1 are not so sharp and for a given H the transition temperature is about 1.5 K lower than that of GdAs No. 2. Another important feature is that an anomalous broad peak is observed at the temperature much below the Néel point in both samples, which can be seen more clearly in the plot C/T versus T^2 (see inserts of Figs. 7 and 8). The position of this broad peak is around 5.5 K and no clear differences is found between the two samples. It is mysterious that even though a magnetic field is applied up to 10 T the position of this broad peak does not change in both samples. In fact, we have observed the similar broad peaks in all Gd-monopnictides GdX (X=N, P, As, Sb, and Bi).[8] Thus it is a common feature existing in Gd monopnictides. Figure 9 shows the temperature dependence of the entropy at zero field for GdAs No. 1 and GdAs No. 2. Above T_N the entropy slowly increases still in both samples and exceeds R ln8, the value expected from the ground state $^8S_{7/2}$. The reason may be mainly the residual phonon contribution, because we used the data of $(C_{\mathrm{LaAs}}+C_{\mathrm{LuAs}})/2$ as the phonon part of specific heat in both GdAs No. 1 and GdAs No. 2, which may be too

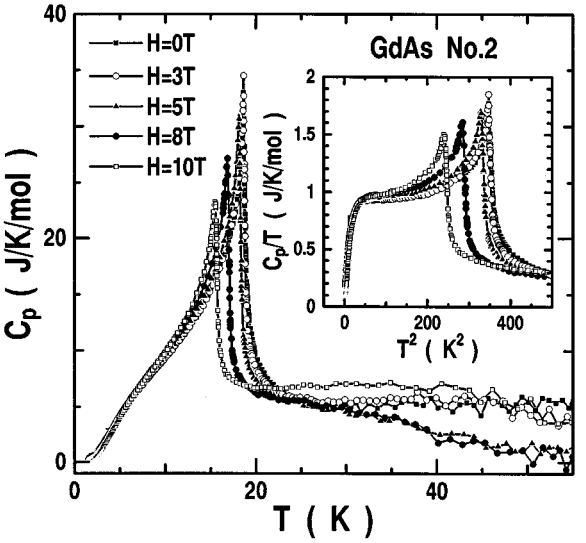

FIG. 8. Temperature dependence of the magnetic part of the specific heat of GdAs No. 2 in magnetic fields of 0, 3, 5, 8, and 10 T. The inset shows the behavior of C_P/T versus T^2.

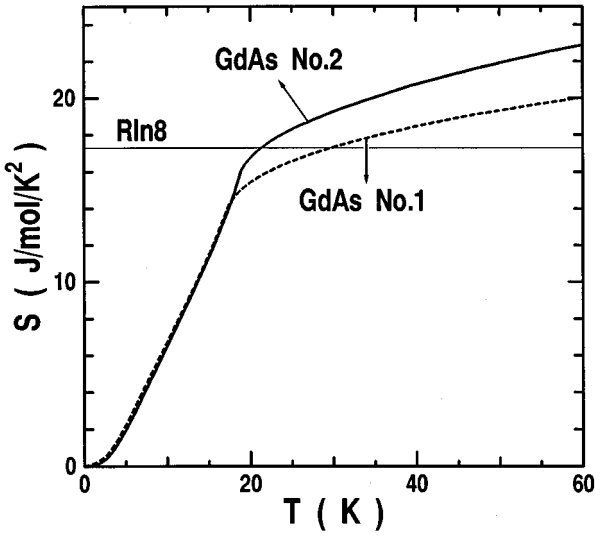

FIG. 9. Entropies of GdAs No. 1 and GdAs No. 2 at zero field.

small for GdAs. Above Néel temperature T_N, the entropy in GdAs No. 2 is larger than that in GdAs No. 1. At $T=T_N$, the entropy in GdAs No. 1 is about 1/10 smaller than that in GdAs No. 2. This value corresponds to $M_s/10$, the value of spontaneous moment, existing in nonstoichiometric sample GdAs No. 1 at zero field as described above.

Finally, the magnetic phase diagrams of the two samples are shown in Fig. 10, which are obtained from the specific heat and magnetization measurements. The left and the right sides of each curve represent the canted and the paramagnetic phases of corresponding sample, respectively. The pure antiferromagnetic phase in stoichiometric sample GdAs No. 2 exists below 0.16 T.

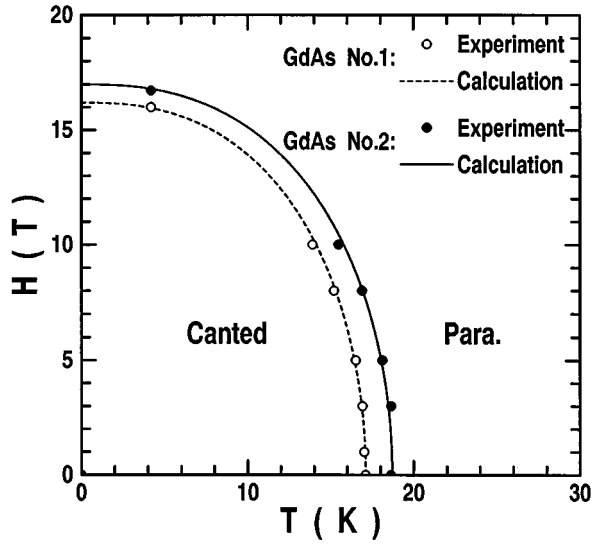

FIG. 10. H-T phase diagram for GdAs No. 1 and GdAs No. 2 obtained from the specific heat measurement ($T>13$ K) and magnetization measurement ($T=4.2$ K). The solid and dashed lines are the curves of $T(H)=T_N(0)[1-(H/H_C)^2]^{0.4}$.

IV. DISCUSSION

The magnetic properties of Gd monopnictides have been investigated by several authors. Neutron diffraction experiments revealed that an antiferromagnetic fcc type-II order exhibits in GdP,[9] GdSb (GdBi),[10] and probably in GdAs.[11] Susceptibility measurements by Busch *et al.*[12] and by McGuier *et al.*[10] gave the Néel temperature values of GdAs to be 25 and 19 K, respectively. While the value of $T_N=13$ K was given by Sugawara *et al.*[13] from their EPR measurements. In the present study, both the susceptibility and specific heat measurements yield the Néel temperature of stoichiometric GdAs No. 2 to be 18.7 K. This value is close to the data obtained by McGuier *et al.* but differs from the result obtained by Busch and Sugawara *et al.* In fact, the Néel temperature depends on the purity of samples. For our stoichiometric sample GdAs No. 2, the transport properties measurements suggest that this sample is a high quality single crystal of antiferromagnetic semimetal with a good compensation between electrons and holes.[8] Thus the experimental results for this sample respond to the intrinsic features of pure GdAs. On the other hand, chemical analysis showed that GdAs No. 1 is a Gd-rich nonstoichiometric sample. Thus some vacancies of As atom exist in GdAs No. 1. Around these vacancies, the so-called trapped magnetic polaron states can be formed, which strongly affect the magnetic and transport properties of the sample. In the following, we will first discuss the general behavior of the samples with molecular field approximation and then explain the anomalous magnetic properties observed in nonstoichiometric GdAs No. 1 with trapped magnetic polaron model.

A. General features

1. Magnetization

As is shown in Fig. 3, for GdAs No. 2, two peaks are observed in the curve of derivative dM/dH at a lower field $H_{\rm sf}$ and a higher field H_C, which represent the phase transition from antiferromagnetic phase to spin-flop phase and from spin-flop phase to paramagnetic phase, respectively. The spin-flop transition theory has been reviewed earlier by Shapira[7] for the case of a uniaxial antiferromagnet of the easy-axis type. According to this theory, if a magnetic field $\boldsymbol{H}$ is applied along $\pm\boldsymbol{n}$, where $\pm\boldsymbol{n}$ are the unit vectors of the sublattice magnetizations $\boldsymbol{M}_1$ and $\boldsymbol{M}_2$, at a certain value of $H=H_{\rm sf}$, $\boldsymbol{M}_1$ and $\boldsymbol{M}_2$ will rotate abruptly to the directions which are nearly perpendicular to $\boldsymbol{H}$. This rotation process is known as the spin-flop transition, and the two phases below and above $H_{\rm sf}$ are called antiferromagnetic phase and spin-flop phase, respectively. At $H_{\rm sf}$ the curve of dM/dH has a sharp peak. Pure GdAs is a cubic antiferromagnet with magnetic order of type II, thus the four equivalent {111} planes are the easy planes for the sublattice magnetizations. At zero field and below T_N, $\boldsymbol{M}_1$ and $\boldsymbol{M}_2$ are antiparallel with each other and point along the certain directions. When a magnetic field is applied and at a certain value, $H_{\rm sf}$, the sublattice magnetizations $\boldsymbol{M}_1$ and $\boldsymbol{M}_2$ should rotate in the {111} planes toward the directions which are nearly perpendicular to $\boldsymbol{H}$. This process is analogous to the spin-flop transition in uniaxial antiferromagnet as mentioned above despite the fact that GdAs is not a uniaxial antiferromagnet. The spin-flop transition field $H_{\rm sf}$ in GdAs No. 2 is evaluated to be 0.16 T from Fig. 3. Note that the transition peak around $H_{\rm sf}$ in GdAs No. 2 is not so sharp; the reason may be that the direction of $\boldsymbol{H}$ (applied along [100]) deviates from $\pm\boldsymbol{n}$, so that the tran-

sition should take place gradually as described in Ref. 14. Note also that, at low field, a large peak also appears in the dM/dH curve of GdAs No. 1; this peak represents a weak ferromagnetic transition other than a spin-flop transition.

According to the uniaxial antiferromagnet theory, in spin-flop phase the sublattice magnetizations $\boldsymbol{M}_1$ and $\boldsymbol{M}_2$ are canted relative to each other by an angle. As H increases the canting angle increases until $\boldsymbol{M}_1$ and $\boldsymbol{M}_2$ become parallel relative to each other and to $\boldsymbol{H}$, while a second-order phase transition from spin-flop phase to paramagnetic phase happens. This transition is also observed in both GdAs No. 1 and GdAs No. 2 at $H_C=16$ and 16.7 T, respectively. The values of these critical fields H_C are slightly lower than the values of saturation fields described in Sec. III. The former represents the starting of the transition and the latter represents the finishing of the transition. The transition field $H_C(T=0)$ can be related to the exchange constants J_1 and J_2 (see the following). For an fcc antiferromagnet with a second-kind order, the MFA gives $H_C(T=0)=-84(J_1+J_2)/(g\mu_B)$. Using this formula $H_C(T=0)$ of GdAs is calculated to be 15.0 T. This value is slightly lower than the obtained experimental data.

Above 3 T the derivative dM/dH of GdAs No. 2 increases slowly with increasing H, in disagreement with MFA which predicts a constant susceptibility in the canted phase. Similar effect was observed earlier by Jacobs *et al.*[15] and Oliveira *et al.*[16] in EuTe and was attributed primarily to the zero-point spin-wave contributions to the free energy.

2. Susceptibility

According to MFA theory, at $T<T_N$ and $H<H_{sf}$, susceptibility of an antiferromagnetic single crystal is given by $\chi(\theta)=\chi_{\parallel}\cos^2\theta_+\chi_{\perp}\sin^2\theta$, where θ is the angle between the directions of $\boldsymbol{H}$ and $\boldsymbol{n}$ and $\chi_{\parallel}$ and $\chi_{\perp}$ are the parallel and perpendicular susceptibilities, respectively. The $\chi_{\perp}$ is temperature independent below T_N and is equal to $\chi_{\max}$. $\chi_{\parallel}$ is expected to vanish at $T=0$ and increases with T. At T_N, $\chi_{\parallel}=\chi_{\perp}=\chi_{\max}$, and above T_N, the magnet becomes a paramagnet and the susceptibility obeys the Curie-Weiss law. Our measurements for GdAs No. 2 in a field of 0.05 T show that the susceptibility is approximately equal to $2/3\chi_{\max}$ at lowest temperature and increases with T. After going through a maximum just above T_N, χ becomes Curie-Weiss-like at higher temperatures. These results are in agreement with the MFA as described above.

The exchange interaction between magnetic ions in GdAs can be described in terms of an interaction of each Gd^{3+} ion with its 12 nearest neighbors and six next-nearest neighbors. The next-nearest-neighbor interaction is antiferromagnetic and is stronger than the nearest-neighbor interaction which is ferromagnetic. For GdAs (face-centered-cubic lattice with type-II magnetic ordering and $J=7/2$) the experimental values of T_N and θ_P can be used to evaluate the nearest-neighbor exchange constants J_1 and the next-nearest-neighbor exchange constant J_2 by using the following equations:

$$k_B T_N=-63J_2, \tag{1}$$

$$k_B\theta_P=126J_1+63J_2. \tag{2}$$

For stoichiometric sample of GdAs No. 2, let $T_N=18.7$ K and $\theta_P=-11.5$ K, we find $J_1=0.06$ K and $J_2=-0.30$ K. The antiferromagnetic next-nearest-neighbor interaction J_2 is stronger than the ferromagnetic nearest-neighbor interaction J_1; this is the general feature for a Heisenberg antiferromagnet. In fact, we have measured the susceptibilities and calculated the exchange constants J_1 and J_2 for all stoichiometric Gd monopnictides. J_1 and J_2 show the regular changes when going from GdN to GdBi. For nonstoichiometric GdAs No. 1, since the magnetic polarons make a contribution to the susceptibility (as explained in the following), Eq. (2) is no longer valid.

We will elaborate the mechanism of exchange interaction in pure Gd monopnictides in a separate paper. As the conclusions, in GdAs (and other Gd monopnictides), an indirect cation-cation exchange with virtual transfer of a $4f$ electron to the $5dt_{2g}$ excited state of a neighboring cation is responsible for the ferromagnetic exchange J_1, and the d-f superexchange mechanisms account for the antiferromagnetic exchange J_2 ($|J_2|>J_1$) similar to the case of europium chalcogenides which has been studied by Kasuya.[17] But the essential distinctions between Eu chalcogenides and Gd monopnictides are that Eu chalcogenides are semiconductors while Gd monopnictides are semimetals, thus the d-f exchange in Eu chalcogenides can only work through the virtual transfer of the anion p electrons to a $5d$ or $6s$ states. Due to the existence of free carrier, an additional Ruderman-Kittel-Kasuya-Yosida (RKKY) interaction is superimposed on the antiferromagnetic superexchange interaction in Gd monopnictides. On the other hand, the separation of the $4f$ level and the $5d$ band is 2–3 eV in Eu chalcogenides and 7–10 eV in Gd monopnictides; thus the d-f mixing term is proved to be responsible for J_1 in a good agreement with the experiment of Eu chalcogenides, but it is not important in Gd monopnictides. In nonstoichiometric sample GdAs No. 1, due to the formation of trapped magnetic polaron state, it exhibits weak ferromagnetic properties at low fields as discussed in the following.

3. Specific heat under magnetic fields

The quantitative calculation of specific heat as a function of temperature and magnetic field for an antiferromagnet is very difficult. In fact, up to now, there is not satisfactory theory of the $C(T,H)$ calculation for an antiferromagnet in the canted phase. Only a few attempts were made to calculate the thermodynamic properties in the case of zero field or very low temperatures.[18] Thus the origin of the broad peak of the specific heat around 5.5 K in GdAs cannot be explained very clearly now. Since a similar broad peak exists in all Gd monopnictides and some other Gd compounds, it seems, therefore, that this broad peak is an intrinsic feature of S-state ion, and further study is necessary.

The phase boundaries of antiferromagnet have been calculated by several authors with different models. Our specific heat measurements show the transition (from the spin-flop phase to the paramagnetic phase) temperature decreases slowly with the applied field. This is the typical feature of antiferromagnetism and can be explained qualitatively with the MFA model. In MFA, if $H_A \ll 2H_E$, which is case for GdAs, then $H_C \approx 2H_E$,[16] where H_A is the effective anisotropy field and H_E is the intersublattice exchange field. Be-

cause H_E is proportional to the sublattice magnetization M_i ($i=1$ or 2), the field dependence of the transition temperature is given by H dependence of the sublattice magnetization M_i. Since M_i decreases slowly with increasing H near T_N, the transition temperature shifts to low temperature with increasing H. The specific heat measurements yield a phase diagram as shown in Fig. 10, which can be fitted fairly well by an expression of the form

$$T(H)=T_N(0)[1-(H/H_C)^2]^{\xi}, \tag{3}$$

where $\xi=0.40$ is chosen for GdAs. Formula (3) had been used earlier to describe the Ising ferromagnets and antiferromagnets with $\xi=0.87$, 0.35, and 0.36 for the square, simple cubic, and bcc lattices, respectively.[19]

B. Effect of trapped magnetic polaron state

We have systematically described the difference between the magnetic properties in stoichiometric sample GdAs No. 2 and those in nonstoichiometric sample GdAs No. 1. The magnetic properties of GdAs No. 2 can be understood with the Heisenberg antiferromagnetic theory as analyzed above. Compared with GdAs No. 2, nonstoichiometric GdAs No. 1 shows quite anomalous features which can be explained by the trapped magnetic polaron model.[20] Due to the nonstoichiometry, the As atom vacancies exist in GdAs No. 1 sample. We show two possible mechanisms of how the electrons originated from these vacancies can cause weak ferromagnetism at zero field. One mechanism is the trapped magnetic polaron effect. The basic idea is the following: because of the Coulomb potential at the vacancies, some of the electrons originated from the vacancies are trapped at the sites of the As atom vacancies, and interact strongly with the surrounding $4f$ spins through d-f exchange interaction which cause the $4f$ spins around the trapped electron to be aligned, i.e., trapped magnetic polaron states are formed. A second mechanism is that a fraction of the electrons originated from the vacancies enters the conduction band and freely moves through the lattice so as to cant all the $4f$ electron spins uniformly through the lattice. Both mechanisms can lead to a spontaneous magnetic moment at zero field. It is known that in low-carrier concentration systems the trapping magnetic polaron mechanism is important.[21] This is also true for GdAs.

At low fields, with increasing magnetic field, the nonlinear and rapid increase of magnetization of GdAs No. 1 indicates the existence of spontaneous magnetic moments or weak ferromagnetism which is mainly originated from the trapped magnetic polar states. When an external magnetic field $\boldsymbol{H}$ is applied, the spontaneous magnetic moments of polarons align themselves parallel to $\boldsymbol{H}$, even at low fields. This lead to the rapid increase of magnetization and the large values of magnetic susceptibility in GdAs No. 1 at low fields and low temperatures. Figure 6 clearly shows that the large susceptibility difference between nonstoichiometric and stoichiometric GdAs samples is present at only lower temperatures. Since this susceptibility difference disappears above 200 K, the trapped magnetic polaron states formed in GdAs No. 1 are considered to be disintegrated above 200 K.

The smaller entropy value observed in GdAs No.1 is another evidence of the formation of trapped magnetic polaron states in this sample. At $H=0$ and $T=T_N$, the entropy in GdAs No. 1 is smaller than that in GdAs No. 2, and the entropy difference is about 1.8 J mol^{-1}K^{-2}. This value is about R ln8/10 and corresponds to $M_S/10$, the value of spontaneous moment which exists in nonstoichiometric sample GdAs No. 1 at zero field. Since we use the same specific heat date for the phonon contribution in both GdAs No. 1 and GdAs No. 2, thus the smaller entropy in GdAs No. 1 is considered to mainly due to the trapped magnetic polaron effect. That is, because the long-range magnetic order coexists with the trapped magnetic polarons even at T_N, about 1/10 $4f$ spins do not participate in the long range order, and keep the ferromagnetic order within the polarons.

Further evidence of the formation of trapped magnetic polaron states in GdAs No. 2 is the large negative magnetoresistance at low temperature and low magnetic field and the anomalous temperature dependence on the electric resistively, which will be discussed together with the other transport properties in a separate paper.[8] Similar anomalous magnetic and transport properties have also been found in our other nonstoichiometric gadolinium monopnictides samples, such as GdP, which can also be understood with the same trapped magnetic polaron model.

It is well known that trapped magnetic polaron effect is evident only in some low carrier systems, i.e., in some strongly correlated electron systems. Among them, Eu chalcogenides, another series of S-state $4f$ compounds, have been investigated extensively. Because of fairly weak crystalline electric field effect, the strong exchange interaction is the main mechanism of magnetic properties in both Gd monopnictides and Eu chalcogenides. It is believed that the trapped magnetic polaron states can be easily formed and have strong effects on magnetic and transport properties of Gd monopnictides and Eu chalcogenides. In fact, the clear magnetic polaron effects have been found in nonstoichiometric EuTe,[16,21,22] and other Eu chalcogenides.[23] Some other magnetic semiconductors containing carriers such as Gd$_{3-x}$V$_x$S$_4$ also shown this kind of behavior.[24] However, as far as we know, the evident trapped magnetic polaron effects are discovered in semimetal Gd monopnictids in the present work. One question one may ask is what are the differences between Gd monopnictids and Eu chalcogenides? First, the carrier concentrations are different. Eu chalcogenides are magnetic semiconductors; even in Eu-rich EuTe, its carrier concentration ($\sim 10^{19}/\mathrm{cm}^3$) is much lower than that in semimetal GdAs ($\sim 10^{20}$–$10^{21}/\mathrm{cm}^3$).[8] Thus the trapped magnetic polaron states in Eu chalcogenides are considered to be formed more easily and stably than that in Gd monopnictids. As described above, in low carrier concentration systems, because the trapping magnetic polaron mechanism is much important than the uniformly canted lattice spins effect, one believes that in Eu-rich EuTe, only the trapped magnetic polaron states are formed, and very little or no uniform-spin canting exists in zero field due to the very low carrier concentration. Thus both Eu-rich EuTe (which shows trapped magnetic polaron effect) and pure EuTe (with no trapped magnetic polaron effect) should have the same Néel temperature. This has been proved by the experiments.[16] However, in nonstoichiometric GdAs, although the formulation of the trapped magnetic polaron states is still the main mechanism, the uniform-spin canting can also be formed due to the rela-

tively higher carrier concentration and thus the stoichiometric and nonstoichiometric GdAs samples should show different Néel temperatures. This difference has also been observed in the present work: the Néel temperatures (GdAs No. 1: 17.2 K; GdAs No. 2: 18.7 K) obtained from the susceptibility and specific heat measurements show a clear difference of 1.5 K between stoichiometric GdAs No. 2 and nonstoichiometric GdAs No. 1 samples. Secondly, the exchange mechanisms are quite different. Although trapped magnetic polaron states are formed through d-f interaction in both EuTe and GdAs, in the former d-f exchange can only work through the virtual transfer of the anion p electrons to $5d$ or $6s$ states, and d-f mixing is also important. In the later d-f mixing can be ignored due to deep $4f$ level, and an additional RKKY interaction is also important as discussed above. A defect of tellurium atom in EuTe is a doubly charged donor, whereas a defect of an arsenic atom in GdAs is a triply charged donor. The former case has recently been investigated by Umehara[25] in a He-like model with singlet or triplet spin configurations of impurity electrons. Such a model is not suitable for GdAs, because of the different electron spin configuration. It is clear that further theoretical and experimental studies are necessary for a more detailed understanding of the trapped magnetic polaron states in nonstoichiometric GdAs and other Gd monopnictides.

It is interesting to note that a new type of magnetic polaron theory (different from the above trapped magnetic polaron model), i.e., the quasilocalized p hole polarizes the $4f$-Γ_8 state through the strong Γ_8 p-f mixing interaction, has recently been developed by Kasuya to explain the various anomalous physical properties observed in stoichiometric Ce and Yb monopnictides.[5,26,27] These kinds of anomaly (such as stronger temperature dependence of Hall coefficient in CeAs, etc.) are not observed in stoichiometric GdAs and other Gd monopnictides. Thus this type of magnetic polaron states could not be formed in stoichiometric Gd monopnictides. The reason may be that the p-f mixing interaction is very weak in Gd monopnictides due to their deep $4f$ levels.

In conclusion, magnetic properties of stoichiometric and nonstoichiometric GdAs single crystals are found to be very different. The stoichiometric sample GdAs No. 2 shows the magnetic behavior expected for a Heisenberg antiferromagnet and can be understood with molecular field approximation. The nonstoichiometric sample GdAs No. 1 shows the anomalous magnetic features, which can be explained by trapped magnetic polaron model.

ACKNOWLEDGMENT

We would like to thank Dr. M. Umehara for helpful discussion.

*Present address: Suzuki Laboratory, Institute for Materials Research, Tohoku University, Katahira 2-1-1, Aoba-ku, Sendai 980-77, Japan.

[1] T. Kasuya, J. Alloys Comp. **192**, 217 (1993).
[2] T. Kasuya, Y. Haga, Y. S. Kwon, and T. Suzuki, Physica B **186-188**, 9 (1993).
[3] T. Kasuya, Y. Haga, T. Suzuki, Y. Kaneta, and O. Sakai, J. Phys. Soc. Jpn. **61**, 3447 (1992).
[4] T. Kasuya, A Oyamada, M. Sera, Y. Haga, and T. Suzuki, Physica B **199-200**, 585 (1994).
[5] T. Kasuya, J. Phys. Soc. Jpn. **63**, 843 (1994).
[6] T. Kasuya, J. Alloys Comp. **192**, 11 (1993).
[7] Y. Shapira, J. Appl. Phys. **42**, 1588 (1971).
[8] D. X. Li, Y. Haga, H. Shida, and T. Suzuki (unpublished).
[9] N. Nereson and V. Struebing, in *Magnetism and Magnetic Materials, 1971 (Chicago)*, Proceedings of the 17th Annual Conference on Magnetism and Magnetic Materials, edited by C. D. Graham, Jr. and J. J. Rhyne, AIP Conf. Proc. No. 5 (AIP, New York, 1972), p. 1385.
[10] T. R. McGuire, R. J. Gambino, S. J. Pickart, and H. A. Alperin, J. Appl. Phys. **40**, 1009 (1969).
[11] F. Hulliger, in *Handbook on the Physics and Chemistry of Rare Earths, Vol. 4*, edited by K. A. Gschneidner, Jr. and L. R. Eyring (North-Holland, Amsterdam, 1979), p. 191.
[12] G. Bush, O Vogt, and F. Hulliger, Phys. Lett. **15** 301 (1965).
[13] K. Sugawara. C. Y. Huang, and D. L. Huber, J. Low Temp. Phys. **26**, 525 (1977).
[14] H. Rohrer and H. Thomas, J. Appl. Phys. **40**, 1025 (1969).
[15] I. S. Jacobs and S. D. Silverstein, Phys. Rev. Lett. **13**, 272 (1964).
[16] N. F. Oliveira, Jr., S. Foner, Y. Shapira, and T. B. Reed, Phys. Rev. B **5**, 2634 (1972).
[17] T. Kasuya, IBM J. Res. Dev. **14**, 214 (1970).
[18] For example, J. Feder and E. Pytte, Phys. Rev. **168**, 640 (1968).
[19] A. Bienenstock, J. Appl. Phys. **37**, 1459 (1966).
[20] S. Methfessel and D. C. Mattice, *Magnetism*, edited by H. P. J. Wijn, Handbuch der Physik Vol. 18 (Springer-Verlag, Berlin, 1968).
[21] Y. Shapira. S. Foner, N. F. Oliveira, Jr. and T. B. Reed. Phys. Rev. B **5**, 2647 (1972).
[22] J. Stankiewicz, S. von Molnar, and F. Holtzberg, J. Magn. Magn. Mater. **54−57**, 1217 (1986).
[23] S. von Molner and S. Methfessel, J. Appl. Phys. **38**, 959 (1967).
[24] N. Mori, Y. Okayama, H. Takahashi, Y. S. Kwon, and T. Suzuki, J. Appl. Phys. **69**, 4696 (1991).
[25] M. Umehara, Phys. Rev. B **46**, 12 323 (1992).
[26] T. Kasuya and T. Suzuki, J. Phys. Soc. Jpn. **61**, 2628 (1992).
[27] T. Kasuya, T. Suzuki, and Y. Haga, J. Phys. Soc. Jpn. **62**, 2549 (1993).